American Mineralogist, Volume 74, pages 969–980, 1989

Redox equilibria and crystal chemistry of coexisting minerals from spinel lherzolite mantle xenoliths

M. Darby Dyar, Anne V. McGuire
Department of Geological Sciences, University of Oregon, Eugene, Oregon 97403, U.S.A.
Richard D. Ziegler
Department of Geology, St. Lawrence University, Canton, New York 13617, U.S.A.

Abstract

Mössbauer investigation of coexisting phases in spinel lherzolites from localities at Dish Hill and Cima, California, San Carlos, Arizona, Potrillo maar, New Mexico, and Al Kishb, Saudi Arabia, yields new insight into their redox equilibria and crystal chemistry. Olivines in these rocks contain no detectable Fe^{3+}, and Fe^{2+} doublets corresponding to both M1 and M2 octahedral sites are observed in our room-temperature spectra. Spinel spectra are fit with four doublets corresponding to octahedral Fe^{3+}, octahedral or tetrahedral Fe^{2+}, and two further different types of tetrahedral Fe^{2+} sites. Calculation of $\log f_{O_2}$ values based on the measured Fe^{3+} numbers yields values close to the FMQ buffer at 15 kbar, in agreement with existing estimates for Cr-rich diopside group spinel peridotites. Orthopyroxene spectra also display four doublets corresponding to Fe^{2+}_{M1}, Fe^{2+}_{M2} adjacent to divalent M1 sites, Fe^{2+} adjacent to partially trivalent M1 sites, and Fe^{3+} in predominantly octahedral M1 sites. Unusually high disorder of Fe^{2+} is observed in the two specimens from Californian sites in the Basin and Range province and may be related to high heat flow in those regions. Clinopyroxene data show that Fe^{2+} is distributed into both M1 and M2 octahedral sites, whereas Fe^{3+} may be either octahedral or tetrahedral. Measured values of $Fe^{3+}/\Sigma Fe$ in all spinels and pyroxenes are consistent within each compositional range studied. In contrast, calculated Fe^{3+} values based solely on stoichiometry and electron-microprobe measurements are inconsistent and generally inaccurate.

Introduction

Understanding of redox conditions of the Earth's mantle is of utmost importance to petrologists and geochemists studying a variety of mantle-related processes such as mantle-core equilibria, mantle and crustal evolution, and magma genesis. Oxygen fugacities (f_{O_2}) of mantle rocks have often been estimated by direct measurement of intrinsic f_{O_2} (IOF) using an electrochemical cell technique and by thermobarometric calculation of f_{O_2} from mineral assemblages in mantle rocks. IOF measurements yield values on or below the iron-wüstite (IW) buffer for Cr-rich diopside group[1] spinel peridotite, spinel megacrysts, and spinel separated from Cr-rich diopside group peridotites (Arculus and Delano, 1981; Arculus et al., 1984; Ulmer et al., 1987) (Fig. 1). Ilmenite megacrysts from kimberlites and Al-rich augite group spinel peridotites yield IOF measurements within 2 log units of the fayalite-magnetite-quartz (FMQ) buffer (Arculus et al., 1984). This contrast between IOF measurements of Cr-rich diopside group and Al-rich augite group rocks has not been explained.

Recognition of problems with electrochemical IOF measurements (Koseluk et al., 1979; Moats and Ulmer, 1986; Pasteris and Wanamaker, 1988) has encouraged development of thermodynamic calculations to determine mantle f_{O_2}. Oxygen fugacities determined by thermodynamic calculations yield values ranging from the magnetite-wüstite (MW) to FMQ buffers for coexisting ilmenite + spinel assemblages (Haggerty and Tompkins, 1983) and for olivine + orthopyroxene + ilmenite assemblages in peridotite nodules from kimberlites (Eggler, 1983). Mattioli and Wood (1986, 1988) and O'Neill and Wall (1987) calibrated an f_{O_2} thermobarometer for the assemblage olivine + orthopyroxene + spinel. Application of this thermobarometer yields f_{O_2} values between the MW and magnetite-hematite (MH) buffers (Fig. 1), at 15 kbar, for Cr-rich diopside group and Al-rich augite group spinel peridotites (Mattioli and Wood, 1986, 1988; O'Neill and Wall, 1987).

The olivine-orthopyroxene-spinel f_{O_2} thermobarometer shows potential to be a useful tool in studies of mantle-rock redox conditions. However, formulations of the thermobarometer use a number of assumptions that require examination before these calculations can be accepted as reliable indicators of f_{O_2}. The Mattioli-Wood and O'Neill-Wall calculations require knowledge of the

[1] In order to conform to IMA guidelines, terminology for Cr-rich pyroxenes is described with the phrase "Cr-rich diopside group," which is equivalent to "Cr-diopside group" as used by Wilshire and Shervais (1975).

0003–004X/89/0910–0969$02.00

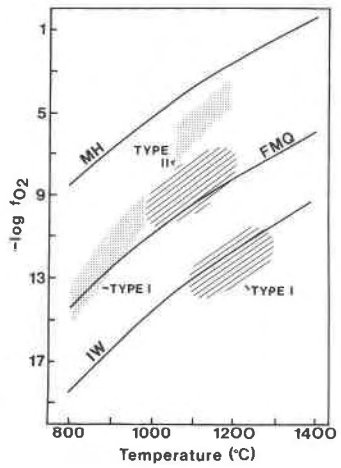

Fig. 1. Published IOF values of spinels from Cr-rich diopside group (Type I) and Al-rich augite group (Type II) spinel peridotites and ilmenite megacrysts (Arculus and Delano, 1981; Arculus et al., 1984), in hatched pattern. Thermobarometric f_{O_2} estimates (at 15 kbar) of Mattioli and Wood (1986) in shaded pattern.

Fe^{2+} content of olivine and orthopyroxene and the Fe^{3+} content of spinel. In most published applications of this f_{O_2} calculation (Mattioli and Wood, 1988; O'Neill and Wall, 1987), all Fe in olivine and orthopyroxene is assumed to be Fe^{2+}, and Fe^{3+} in spinel is calculated from microprobe analyses assuming perfect stoichiometry.

This same set of assumptions regarding Fe^{2+}/Fe^{3+} contents of mantle phases is made for most of the other commonly used geothermometers and geobarometers (e.g., Ellis and Green, 1979; Wells, 1977; Fabries, 1979; Harley, 1984; and many others). In this era of abundant microprobe analysis, with its inability to distinguish Fe^{2+} from Fe^{3+}, few data are available on Fe^{3+} contents of mantle rocks and their constituent minerals. In general, Fe^{3+} is assumed to be zero or neglible in mantle clinopyroxene, orthopyroxene, olivine, and garnet, and Fe^{3+} is calculated for spinel by assuming ideal stoichiometry. To date, few studies (Canil et al., 1988; Wood et al., 1988) have actually measured Fe^{2+}/Fe^{3+} ratios (by using Mössbauer spectroscopy) of spinels from spinel peridotite samples used for f_{O_2} thermobarometry. Those studies did not report measurements of Fe^{2+}/Fe^{3+} in the coexisting pyroxenes and olivine.

This lack of good Fe^{2+}/Fe^{3+} data for mantle rocks may have serious implications for mantle studies. Incorrect assumptions about Fe^{2+}/Fe^{3+} ratios in mantle minerals may lead to large errors in temperatures and pressures estimated by Fe-Mg exchange thermobarometers such as those used in the studies of Ellis and Green (1979), Harley (1984), and Fabries (1979). Interpretations concerning lithospheric structure and evolution are often based on *P-T* estimates using these thermobarometers.

This study was undertaken with the aim of improving knowledge of Fe^{2+}/Fe^{3+} ratios and crystal chemistry of mantle minerals. Mössbauer spectroscopy is an excellent tool for determining Fe^{2+}/Fe^{3+} ratios in minerals (Bancroft, 1973; Marfunin, 1979), as well as determining crystallographic site occupancy of Fe (Bancroft, 1967, 1969/1970); this technique has already been applied to the study of mantle minerals (Ward et al., 1988; Wood et al., 1988; McGuire et al., 1989). We present here the results of a Mössbauer spectroscopic study of olivine, spinel, orthopyroxene, and clinopyroxene from five spinel lherzolite xenoliths from alkali basalts.

Methods

Samples

The five spinel lherzolite xenoliths were selected on the basis of size (to allow sufficient material for mineral separates), minimal contamination by the host basalt, and a desire to sample several mantle-xenolith localities. All samples were collected from alkali basalts. One sample, H30-b2, came from Harrat al Kishb, Saudi Arabia, and the other four xenoliths were from southwestern United States localities: Ba-2-3, Dish Hill, California; Ki-5-31, Cima volcanic field, California; Sc-1-1, San Carlos, Arizona; and Ep-1-13, Potrillo maar, New Mexico. All samples are spinel-bearing lherzolites (clinopyroxene $\geq$ 10 modal percent) belonging to the Cr-rich diopside group (as defined by Wilshire and Shervais, 1975; equivalent to Group I of Frey and Prinz, 1978). The Cima xenolith, Ki-5-31, contains minor plagioclase. Brief petrographic descriptions are given in Appendix 1.

Microprobe analyses

Microprobe analyses of Ba-2-3 were provided, along with the sample, by H. G. Wilshire, U.S. Geological Survey. The other four samples were analyzed at the Smithsonian Astrophysical Observatory, Cambridge, Massachusetts, on a JEOL 733 automated electron microprobe. Routine operating conditions were used: 15-kV accelerating voltage, 20-nA beam current, 30-s count times, and focused beam. Matrix correction was done by Tracor Northern ZAF with natural mineral standards. Analytical errors are 0.2–2.0 relative percent for major elements and 5–20% for minor elements. Multiple analyses were done on each mineral in each xenolith to check for homogeneity. All phases were found to be homogeneous within the microprobe errors. In the exsolved pyroxene of H30-b2, the *host* pyroxene phases were homogeneous in composition. Compositions presented in Tables 1–4 are averages of 5–10 analysis points. Microprobe analyses were used to calculate Fe^{3+} contents of spinel, orthopyroxene, and clinopyroxene, assuming perfect stoichiometry (four cations per six oxygens for pyroxene, and three cations per four oxygens for spinel) and charge balance, in order to provide a basis for comparison with the Mössbauer results.

Mössbauer analyses

Careful sample preparation was required to obtain sufficient quantities of high-purity separates of the four mineral phases (olivine, spinel, orthopyroxene, and clinopy-

TABLE 1. Summary of olivine data

	Dish Hill Ba-2-3	Potrillo maar Ep-1-13	Cima volcanic field Ki-5-31	San Carlos Sc-1-1	Al Kishb H30-b2
SiO_2	39.10	40.53	40.80	41.18	41.67
Al_2O_3	n.a.	0.04	n.a.	0.03	0.01
FeO	10.20	10.30	8.90	9.89	8.19
MgO	48.80	47.92	49.40	49.11	50.49
MnO	0.17	0.14	0.14	0.13	0.06
TiO_2	n.a.	0.03	n.a.	0.04	0.03
Cr_2O_3	n.a.	0.02	n.a.	0.00	0.02
CaO	0.10	0.09	0.07	0.08	0.04
Na_2O	n.a.	0.01	n.a.	0.02	0.01
Ni_2O	0.20	0.37	0.38	0.37	0.40
Sum	98.57	99.45	99.69	100.84	100.92
Cations per four oxygens					
Si	0.978	1.002	1.000	1.002	1.004
Al	0.000	0.001	0.000	0.001	0.000
Fe^{2+}	0.213	0.213	0.182	0.201	0.165
Mg	1.820	1.766	1.805	1.780	1.814
Mn	0.004	0.003	0.003	0.003	0.001
Ti	0.000	0.001	0.000	0.001	0.001
Cr	0.000	0.000	0.000	0.000	0.000
Ca	0.003	0.002	0.002	0.002	0.001
Na	0.000	0.000	0.000	0.001	0.000
Ni	0.004	0.007	0.007	0.007	0.008
Sum	3.022	2.997	3.000	2.998	2.995
Fa (%)	10.50	10.76	9.18	10.15	8.34
I.S. M1	1.13	1.14	1.14	1.13	1.14
Q.S. M1	2.86	2.84	2.90	2.88	2.87
Width M1	0.25	0.25	0.28	0.27	0.24
Area M1 (%)	54	40	74	47	51
I.S. M2	1.16	1.16	1.17	1.16	1.16
Q.S. M2	3.03	3.03	3.06	3.02	3.06
Width M2	0.25	0.27	0.20	0.26	0.24
Area M2 (%)	46	60	26	53	49
Misfit (%)	−0.02	0.00	0.02	0.00	0.01
Uncertainty (%)	−0.01	0.00	0.01	0.00	0.00

TABLE 2. Summary of spinel data

	Dish Hill Ba-2-3	Potrillo maar Ep-1-13	Cima volcanic field Ki-5-31	San Carlos Sc-1-1	Al Kishb H30-b2*
SiO_2	0.00	0.17	0.00	0.30	0.15
Al_2O_3	55.40	59.07	52.68	57.75	42.52
TiO_2	n.a.	0.15	0.05	0.13	0.19
FeO	10.90	10.89	10.92	10.24	11.19
MnO	n.a.	0.08	0.00	0.06	0.10
MgO	21.30	21.01	20.61	21.60	19.16
Cr_2O_3	12.30	8.00	13.93	8.23	24.74
CaO	n.a.	0.01	0.00	0.01	0.01
NiO	0.02	0.39	0.00	0.39	0.22
Sum	99.92	99.77	98.19	98.71	98.28
Fe^{3+} (calculated, %)	16	17	23	24	20
Fe^{3+} (Mössbauer, %)	23	23	33	22	34
I.S. 1	1.11	1.08	1.08	1.11	1.07
Q.S. 1	1.75	1.81	1.64	1.79	2.09
Width 1	0.38	0.39	0.36	0.42	0.61
Area 1 (%)	20	22	20	19	20
I.S. 2	0.90	0.91	0.89	0.91	0.93
Q.S. 2	0.96	1.03	0.90	0.98	0.99
Width 2	0.38	0.39	0.36	0.42	0.61
Area 2 (%)	25	25	23	27	7
I.S. 3	0.86	0.80	0.83	0.86	0.80
Q.S. 3	1.63	1.82	1.58	1.66	1.75
Width 3	0.38	0.39	0.36	0.42	0.61
Area 3 (%)	32	30	24	32	39
I.S. 4	0.29	0.33	0.33	0.30	0.32
Q.S. 4	0.79	0.69	0.82	0.76	0.41
Width 4	0.38	0.39	0.36	0.42	0.61
Area 4 (%)	23	23	33	22	34
Misfit (%)	−0.32	0.10	0.30	−0.36	1.49
Uncertainty (%)	−0.07	0.02	0.03	−0.08	0.11
Cations per four oxygens**					
Si	0.000	0.004	0.000	0.008	0.004
Al (tet)	0.046	0.047	0.057	0.023	0.055
Fe^{2+} (tet)	0.132	0.138	0.130	0.128	0.146
Mn	0.000	0.002	0.000	0.001	0.002
Mg	0.822	0.801	0.813	0.832	0.788
Ni	0.000	0.008	0.000	0.008	0.005
Sum tet	1.000	1.000	1.000	1.000	1.000
Cr	0.252	0.161	0.290	0.168	0.536
Ti	0.000	0.003	0.001	0.003	0.004
Fe^{2+} (oct)	0.046	0.057	0.056	0.041	0.061
Fe^{3+}	0.054	0.054	0.079	0.049	0.087
Al (oct)	1.647	1.725	1.574	1.739	1.315
Sum oct	1.999	2.000	2.000	2.000	1.999

* Mössbauer spectrum of this sample was of extremely poor quality because of the small amount of modal spinel in the sample studied. Values given have large errors, estimated to be ±30–40%, as a result.

** Recalculations based on microprobe data recalculated with Mössbauer data. Alternate site assignments are discussed in text.

roxene). All samples were crushed by hand under acetone (to minimize possible oxidation of Fe). Initial separates were prepared using a Frantz magnetic separator where abundant sample was available; most of the separating was done by hand under a binocular microscope. This task was made more difficult by the similarity in color of the green minerals in these rocks; sorting by morphology was generally required to separate those minerals. Because we were limited to the individual lherzolite hand samples selected for this study, several weeks of work were required to generate the optimal amount of sample (21 mg of FeO per mineral phase) required for production of high-quality Mössbauer spectra (Dyar, 1984). In the case of one sample (H30-b2), modal spinel content was so low that it was impossible to obtain a desirable quantity for Mössbauer measurements. However, the 40 mg of sample that was obtained was run and fit with a similar model so that data could be compared with the other spinels in the study (note the high errors on that particular fit, as shown by the Misfit values given at the bottom of Table 2).

Mössbauer measurements were recorded in 512 channels of the constant-acceleration Austin Science Associates spectrometer located in the Mineral Spectroscopy Laboratory at the University of Oregon. A source of 50–30 mCi ^{57}Co in Pd was used; results were calibrated against α-Fe foil of 6-μm thickness and 99.99% purity. Spectra were fitted using a version of the program STONE (Stone et al., 1984) on IBM and AST personal computers with 80386 processors and math coprocessors. The program uses a Gaussian nonlinear regression procedure with a facility for constraining any set of parameters or linear combination of parameters. Lorentzian line shapes were used for resolving peaks, as there was no statistical justification for the addition of a Gaussian component to the curve shape used.

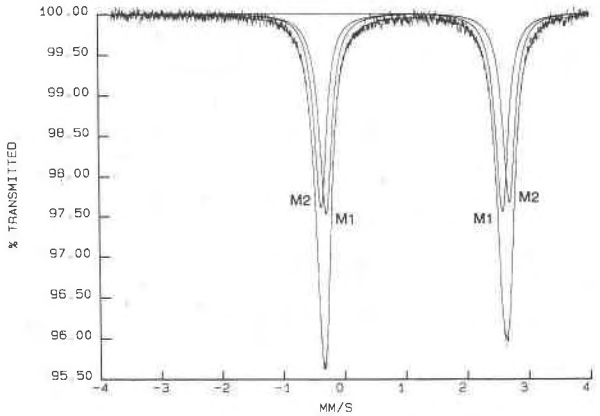

Fig. 2. Typical Mössbauer spectrum of olivine, displaying two narrow doublets approximately equal in size (sample H30-b2).

Fitting procedures were varied depending on the mineral types being examined. Olivine spectra were fit without peak width or area constraints. Clinopyroxene spectra were generally fit with constraints on peak widths only, whereas spinel and orthopyroxene spectra commonly required additional equal-area constraints on the small Fe^{3+} peaks. Careful attention was paid to the location and intensity of the Fe^{3+} peaks in all spectra (except those of olivine, which lacks Fe^{3+}), in order to facilitate correct interpretation of the data. Spectra of spinels and pyroxenes required evaluation of more than 60 different models for each spectrum analyzed. A statistical best fit was obtained for each sample using the χ^2 and Misfit parameters (Ruby, 1973); practical application of these parameters is discussed elsewhere (Dyar, 1984). At best, the precision of the Mössbauer spectrometer and the fitting procedure is approximately ± 0.02 mm/s for isomer shift (δ) and quadrupole splitting (Δ) and $\pm 1.5\%$ per peak for area data in spectra with well-resolved, distinct peaks (Dyar, 1984).

Results

Olivine

Resolution of two doublet fits for all five olivine spectra (Table 1 and Fig. 2) came as a surprise because all samples were run at room temperature; such resolution is generally available only at higher temperatures. Similar room-temperature data have been reported in the literature only on a single natural (mantle) olivine studied by Stanek et al. (1986). In our spectra, the peak widths of the two doublet fits are extremely small—just above the minimum observed width (which is twice the Heisenberg width of 0.097 mm/s). However, peak positions are extremely consistent even though they are unconstrained. The peaks in the M1 doublet fall at $\delta = 1.13$–1.14 mm/s and $\Delta = 2.84$–2.90 mm/s, and the M2 doublet lies at $\delta = 1.16$–1.17 mm/s and $\Delta = 3.02$–3.06 mm/s. These isomer shifts are identical within the precision of the technique, but the different ranges of quadrupole splitting are statistically significant. Site assignment of the doublets as given above is based on the data of Stanek et al. (1986).

Area data on the two doublets (representative of Fe occupancy in the two octahedral sites) are difficult to interpret because the heavy overlap of the two doublets imposes high errors on their relative area determinations. Errors on the areas of the doublets may be as high as $\pm 25\%$. There is also a lack of consensus in the literature on their interpretation. On the basis of differences in point symmetries and geometrical distortions, the M1 and M2 coordination octahedra in olivine are quite distinctive. M1 octahedra share six of twelve edges and are tetragonally distorted (D_{4h} symmetry), whereas M2 octahedra share only three of twelve edges and are trigonally distorted (C_{3v} symmetry). Because the sites are so dissimilar, it might be assumed that Fe^{2+} and Mg^{2+} would order into different sites. In keeping with such assumptions, enrichment of Fe^{2+} into M1 was observed by Bush et al. (1970) and Finger and Virgo (1971). However, later workers (Brown, 1982; Lumpkin and Ribbe, 1983; Stanek et al., 1986) observed only random ordering of Fe^{2+} in olivine, even at high pressures (Stanek et al., 1986). Data produced in this study substantiate both models. Three of the olivine spectra (Ba-2-3, Sc-1-1, and H30-b2) have roughly equal areas of Fe^{2+} peaks within the errors of the measurement, implying random site occupancy of Fe^{2+} (Fig. 2). Two other samples, Ki-5-31 from Cima and Ep-1-13 from Potrillo maar, display 3:1 and 3:2 enrichments (respectively) in M1 over M2. Since all of the olivines have nearly identical compositions, the observed differences in Fe^{2+} occupancy are probably related to thermal history.

Spinel

Interpretation of Mössbauer spectra of spinel phases is complex and frequently disputed. A brief review of the primary viewpoints on spinel structure should prove useful in comprehension of the results of this study.

It is well known that the $(A)[B_2]O_4$ structure of spinel occurs in two types: *normal* spinels, where divalent cations occupy tetrahedral A sites and trivalent cations occur in octahedral B sites, and *inverse* spinels, where trivalent cations occur in fourfold coordination and both divalent and trivalent cations can be found in sixfold B sites. Most spinels of geologic interest have high total Fe contents, such as the end-members magnetite (Fe_3O_4, an inverse spinel), hercynite ($Fe^{2+}Al_2O_4$, a normal spinel), and chromite ($Fe^{2+}Cr_2O_4$, also normal). Although the relative site occupancies of these end-member compositions are fairly well understood, cation distributions in spinels of intermediate compositions are relatively poorly understood. Natural spinels from mantle peridotites may be approximated by the system spinel ($MgAl_2O_4$ end-member)–hercynite–chromite–magnetite, with trace amounts of Ti, Mn, Ni, Zn, and V.

Mössbauer spectra of spinel phases in our samples display four spinel doublets representing both octahedral- and tetrahedral-site occupancies as listed in Table 2 and

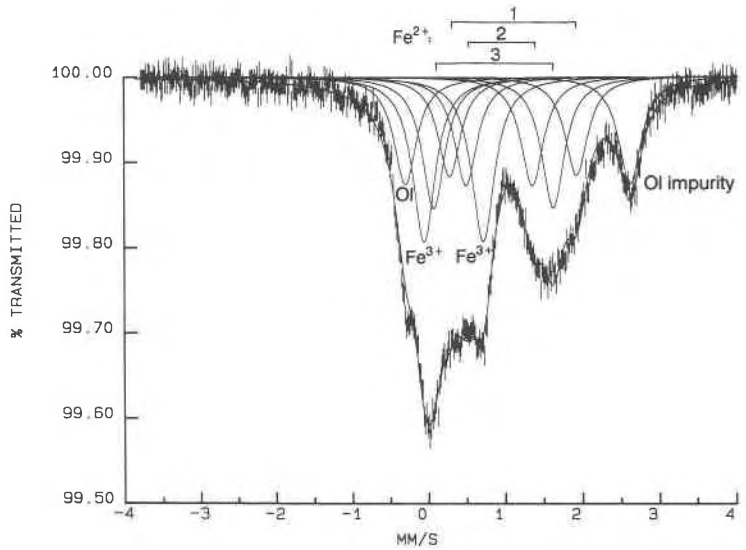

Fig. 3. Spinel spectrum of sample Ki-5-31. The outermost doublet represents a contribution from an olivine impurity that we were unable to eliminate from the spinel separates. Spinel peaks represent Fe^{2+} in both tetrahedral and octahedral coordination and a small amount of octahedral Fe^{3+}.

shown in Figure 3; an additional outer doublet representing an olivine impurity is also present. Interpretation of these spinel spectra is extremely difficult because the peaks are heavily overlapping and of similar areas. Two different site assignments for octahedral Fe^{3+} and octahedral or tetrahedral Fe^{2+} can be made for any given fit depending on how the component peaks are matched up. All spectra in this study have peaks of roughly equal areas at or near (a) −0.10 mm/s, (b) 0.23 mm/s, (c) 0.69 mm/s, and (d) 1.99 mm/s. One model would match peaks (a) and (c) as an octahedral Fe^{3+} doublet (δ = 0.30 mm/s and Δ = 0.79 mm/s) and (b) with (d) as an octahedral Fe^{2+} doublet (δ = 1.11 mm/s and Δ = 1.76 mm/s). This model yields parameters for the Fe^{3+} doublet that are consistent with previous work (Spencer and Schroeer, 1974; Grandjean and Gerard, 1981) and agrees with earlier observations of disordered distribution of Fe^{3+} and Fe^{2+} in both octahedral and tetrahedral sites (Da Silva et al., 1976, 1980; Fatseas et al., 1976).

A second model for interpreting these spectra would pair peaks (a) and (d) (δ = 0.95 mm/s and Δ = 2.09 mm/s) and (b) and (c) (δ = 0.46 mm/s, Δ = 0.46 mm/s). The (a)–(d) doublet would then be assigned to *tetrahedral* Fe^{2+}, whereas the (b)–(c) doublet would still represent octahedral Fe^{3+}. This model is preferred by Wood et al. (1988) and yields Fe^{2+} peaks consistent with studies on Cr spinels (Osborne et al., 1981; Bancroft et al., 1983; Osborne et al., 1984). The latter group of studies concentrated on synthetic samples that were purely Fe^{2+}-bearing and on natural samples from mid- and shallow-level crustal intrusive rocks that have experienced relatively slow cooling rates. Those results show no evidence in any sample for either tetrahedral Fe^{3+} or octahedral Fe^{2+}; all spinels studied were completely ordered normal spinels. However, Osborne and coworkers could not address the problem of site occupancies of complex natural spinels that have quenched from *high* temperature, as is the case with mantle xenoliths. The present study has the advantage of known (and similar) provenances for all samples studied. Although the spinels from lherzolites in this study fall within the compositional range of spinels studied by Osborne et al. (1981), the thermal histories of the spinels in this study are radically different, as they came from depths of at least 30–40 km. It might be expected that spinels equilibrated at and then quenched from high temperatures in the mantle would be more disordered, as originally proposed by Navrotsky and Kleppa (1967, 1968). Therefore, direct comparison of our results with those of Osborne et al. (1981) may not be appropriate because of the effect of temperature on ordering in the spinels.

The data base in this study (five samples), while providing consistent peak positions, is insufficient to definitively favor either of these models. For the purposes of tabulation we have chosen to use the first of the two models discussed, primarily because the Fe^{3+} parameters of the second model are inconsistent with previous work and the thermal history of our samples favors a disordered model. It should be strongly stressed that the errors on the Mössbauer parameters in these spinel fits are at least ±0.04 mm/s, whereas errors on peak areas are ±6%; both errors are significantly higher than those stated above for the other minerals in this study.

All samples in this study do contain unquestionable tetrahedral Fe^{2+} doublets in addition to those discussed above, with δ = 0.89–0.93 mm/s and Δ = 0.90–1.03 mm/s. A fourth spinel doublet fitted to our spectra, with parameters of δ = 0.80–0.86 mm/s and Δ = 1.58–182 mm/s, poses further problems for understanding our data (and spinel spectra in general). The difficulty in interpretation is based on a choice between two contradictory assign-

ments of the fourth doublet. Early workers in spinel spectroscopy interpreted a doublet with δ falling in the range of 0.67–0.80 mm/s to be representative of mixed-valence phenomena where an exchange of electrons between adjacent sites is initiated by thermal exchange. Such mixed-valence species, typical of those broadly called charge-transfer transitions, involve delocalization of electrons between continuous arrays of sites (as in magnetite) or within finite clusters of equivalent cations (see Burns, 1981, or Amthauer and Rossman, 1984, for a good summary of such phenomena). Mössbauer spectra of such materials show a distinct doublet with δ and Δ values intermediate between those of Fe^{2+} and Fe^{3+}; a charge-transfer doublet representing an averaged valence state of $Fe^{2.5+}$ is observed. Values of $\delta = 0.67$–0.76 and $\Delta = 1.36$–1.70 are typical of $Fe^{2.5+}$ doublets (Nolet and Burns, 1979). Early Mössbauer spectra of spinels other than magnetite were interpreted to contain doublets corresponding to such electron hopping (Fatseas et al., 1976; Da Silva et al., 1976, 1980; Van Diepen and Lotgering, 1977). More recent work by Osborne and coworkers suggests an alternate explanation for the ambiguous fourth doublet. Their studies of Cr-bearing spinels show only tetrahedral Fe^{2+} and octahedral Fe^{3+} (Osborne et al., 1981). By utilizing partial quadrupole splitting theory (Bancroft et al., 1983), they suggested that an extra Fe^{2+} doublet with different quadrupole splitting may be fit to represent a group of tetrahedra with slightly different next-nearest-neighbor configurations instead of a charge-transfer doublet.

Correct interpretation of the fourth doublet with $\delta \simeq 0.82$ mm/s is important to this study because its assignment makes a dramatic difference in Fe^{3+}/Fe^{2+} ratio. If the doublet is interpreted as a charge-transfer component, then half its area can be loosely assigned to Fe^{3+} and half to Fe^{2+}. If the doublet is alternatively interpreted to represent additional tetrahedral Fe^{2+}, then its whole area can be assigned to Fe^{2+}.

We choose to accept the latter interpretation of the fourth doublet, that is, as a representation of a different kind of next-nearest-neighbor environment around a tetrahedral Fe^{2+}. Lacking high-temperature Mössbauer data that might dispute this assignment, the tetrahedral Fe^{2+} model is preferred on the basis of isomer-shift data. Our fourth doublet has isomer shifts ranging from 0.80 to 0.86 mm/s; we have noted that the least constrained models fit to our data have δ values at the high end of that range. Those values appear to be too high when compared to the $\delta = 0.67$–0.76 mm/s values for charge transfer doublets. Fortuitously, this interpretation also facilitates unambiguous assignment of site occupancies of Fe, which would not be possible if $Fe^{2.5+}$ charge-transfer doublets were involved.

Therefore we conclude that the Fe atoms in the five lherzolite spinels studied are distributed as follows: all Fe^{3+} in octahedral (B) sites (ranging from 22–34% of the total Fe present), roughly one-third of the Fe^{2+} in octahedral sites as well (representing 19–22% of the total Fe), and the remaining Fe as Fe^{2+} distributed in two different types of tetrahedral sites (areas of the olivine impurity peaks have been factored out). Peak areas of the doublets correspond directly to the quantitative occupancies of the different sites because there is no difference in recoil-free fraction between sites (Sawatzky et al., 1968).

This result contradicts the simple method of site assignment conventionally adopted by mantle petrologists, who usually assign Fe^{3+} to octahedral coordination and Fe^{2+} to tetrahedral only (e.g., Fabries, 1979; Sachtleben and Seck, 1981; Press et al., 1986). The site assignments given at the bottom of Table 2 reflect the more realistic Mössbauer data for Fe. In addition, previous Mössbauer measurements on other end-member compositions (e.g., Banerjee et al., 1969; Jensen and Shive, 1973) provide the basis for assignment of Si, Mn, Mg, and Ni to tetrahedral sites, and Cr and Ti to octahedra. Al is distributed into the tetrahedral site until it is full (from 2 to 5% of the total Al); the remaining Al (the majority) is assigned to octahedral sites as described by Da Silva et al. (1980) and Dehe et al. (1975).

Orthopyroxene

Both orthopyroxenes and clinopyroxenes found in mantle rocks have similar Mössbauer spectra by virtue of having essentially the same structure. Fe atoms may be found, in the most general case, in either of the two octahedral sites in the structure (M1 and M2) or in the tetrahedral site in Si-deficient compositions (Virgo, 1972). Numerous studies of synthetic end-member compositions have comprehensively defined the expected ranges for Mössbauer spectra of simple pyroxenes. However, the Mössbauer spectra of natural samples are not so easily understood because of their multicomponent compositions. For this reason, spectra of the orthopyroxenes and clinopyroxenes in our rocks will be considered separately.

Spectroscopy of the orthopyroxenes has been the subject of considerable discussion in the literature since the original work by Ghose (1965) established the strong preference of Fe^{2+} for the octahedral M2 site. Later workers have investigated the temperature dependence of Fe^{2+}-Mg^{2+} cation ordering as a possible geothermometer (Virgo and Hafner, 1969, 1970), but more recent studies have shown that orthopyroxene order-disorder may more realistically be viewed as an indication of cooling history or "geospeedometry" (Besancon, 1981; Anovitz et al., 1988). Mössbauer spectra of orthopyroxenes generally feature at least two Fe^{2+} doublets representing the M1 and M2 octahedral sites (Bancroft et al., 1967; Evans et al., 1967). Fe^{3+} is confined to or strongly enriched in M1 (Kosoi et gal., 1974; Annersten et al., 1978). If spectra are taken at liquid-N_2 temperatures to enhance peak separation, the Fe^{2+}_{M2} doublet can be fitted to two distinct doublets believed to be related to different next-nearest-neighbor site occupancies (Seifert, 1983). Because the present study was focused on the Fe^{3+} content of orthopyroxene, our separates were not analyzed at low temperatures, but we were still able to resolve one Fe^{3+} and three Fe^{2+} doublets in

all but one sample as listed in Table 3 and shown in Figure 4.

All the orthopyroxenes from our spinel lherzolites had roughly identical Fe^{3+} contents of 4–6% of the total Fe; this amount is just above the 2–3% detection limit of the technique. Hyperfine parameters of the Fe^{3+} doublet range from $\delta = 0.33$–0.45 mm/s (typical of octahedral coordination) in four samples. A fifth orthopyroxene from Dish Hill shows no contribution from Fe^{3+} in octahedral coordination but instead contains 10% of the total Fe in a low isomer-shift doublet (0.09 mm/s) suggestive of tetrahedral coordination. Slight asymmetry of Fe^{2+} doublets, which have from 2 to 4% more area in the lower-velocity peaks, suggests that all samples studied may contain small amounts of tetrahedral Fe^{3+} that may not be resolved.

Although it is clear that Fe^{2+} has only two distinct types of octahedral sites to occupy, assignment of three doublets to the structure is somewhat ambiguous. Virgo and Hafner's original paper (1968) assigns the M1 doublet to the pair of peaks with $\delta = 1.00$ mm/s and $\Delta = 2.25$ mm/s; the M2 doublet has $\delta = 0.94$ mm/s and $\Delta = 1.97$ mm/s. More recent spectra reported by Krizhanskiy et al. (1975) and Annersten et al. (1978) identify the M1 doublet as having $\delta = 1.10$ mm/s, while $\Delta = 2.77$ mm/s; a study of 77-K spectra by Seifert (1983) also indicates a large difference (0.5 mm/s) between Δ of M1 and Δ of M2. Peak positions of Fe^{2+} doublets in this study do not correspond to either of these models exactly. We observe one doublet in each spectrum with a high quadrupole splitting that can be unambiguously assigned to Fe^{2+}_{M1}. The other Fe^{2+} doublets reported here have roughly equivalent isomer-shift values (1.13–1.19 mm/s) and two relatively close groups of quadrupole splittings at 1.90–2.06 and 2.18–2.25 mm/s. Since the compositions of these pyroxenes are extremely Mg rich and Mg is known to have a strong preference for M1, the most logical assignment of our remaining two Fe^{2+} doublets would be to different types of M2 sites.

Seifert (1983) has provided a detailed description of the two different types of M2 sites in orthopyroxenes. His work suggests that when trivalent cations such as Fe^{3+} and Al^{3+} substitute into M1 sites, distortion occurs. Thus there are potentially at least two types of M2 sites: Fe^{2+} in M2 surrounded by only divalent cations in M1 (such as Mg), and Fe^{2+} in M2 surrounded by M1 sites containing at least one trivalent substitution. We believe that this interpretation probably explains the two close groups of Fe^{2+} doublets with lower Δ in our samples.

In summary, the Mössbauer spectra of mantle orthopyroxenes contain four doublets total, corresponding to Fe^{2+}_{M1}, Fe^{2+}_{M2} adjacent to divalent M1 sites, Fe^{2+} adjacent to partially trivalent M1 sites, and Fe^{3+} in predominantly octahedral M1 sites. The relative occupancies of the sites vary greatly as the magnitude of Fe^{2+}_{M1} occupancy varies. The two California samples from Dish Hill and Cima have large proportions of all the Fe atoms in the structure in M1 coordination (41 and 48% of the total Fe, respectively) (Fig. 5). In contrast, the other three orthopyroxenes have only minor amounts of Fe as Fe^{2+}_{M1}. This observed difference in ordering between the two groups of samples may be related to subtle changes in composition, but is more likely a function of different thermal histories; this possibility will be considered in the Discussion section.

TABLE 3. Summary of orthopyroxene data

	Dish Hill Ba-2-3	Potrillo maar Ep-1-13	Cima volcanic field Ki-5-31	San Carlos Sc-1-1	Al Kishb H30-b2
SiO_2	55.20	54.13	54.60	54.72	57.02
Al_2O_3	3.20	5.30	4.30	5.26	2.50
FeO	6.20	6.54	5.90	6.31	5.18
MgO	34.20	31.30	33.50	32.08	34.57
MnO	0.00	0.13	0.16	0.11	0.12
TiO_2	0.20	0.13	0.06	0.13	0.10
Cr_2O_3	0.00	0.34	0.48	0.36	0.35
CaO	0.64	0.93	0.80	0.96	0.48
Na_2O	0.00	0.14	0.08	0.12	0.04
Sum	99.64	98.94	99.88	100.15	100.36
	Cations per six oxygens*				
Si	1.904	1.894	1.881	1.890	1.950
Al	0.130	0.219	0.175	0.214	0.101
Fe^{2+}	0.127	0.191	0.124	0.182	0.148
Fe^{3+}	0.051	0.000	0.046	0.000	0.000
Mg	1.758	1.632	1.720	1.652	1.762
Mn	0.000	0.004	0.005	0.003	0.003
Ti	0.005	0.003	0.002	0.003	0.003
Cr	0.000	0.011	0.013	0.010	0.011
Ca	0.024	0.035	0.030	0.036	0.018
Na	0.000	0.009	0.005	0.008	0.003
Sum	4.000	3.998	4.001	3.999	3.998
Wo	1.24	1.88	1.58	1.90	0.91
En	92.08	87.83	91.79	88.35	91.40
Fs	6.68	10.30	6.63	9.75	7.69
Fe^{3+} (calculated, %)	29	0	27	0	0
Fe^{3+} (Mössbauer, %)	6	6	6	6	4
I.S. M1	1.15	1.15	1.15	1.12	1.08
Q.S. M1	2.95	2.89	2.94	2.44	2.86
Width M1	0.30	0.30	0.30	0.31	0.26
Area M1 (%)	41	9	48	11	8
I.S. M2a	1.18	1.19	1.17	1.16	1.16
Q.S. M2a	2.23	2.25	2.18	2.18	2.14
Width M2a	0.31	0.35	0.30	0.31	0.35
Area M2a (%)	30	54	33	56	87
I.S. M2b	1.13	1.13	1.13	1.13	—
Q.S. M2b	2.01	2.00	1.92	1.91	—
Width M2b	0.31	0.35	0.30	0.31	—
Area M2b (%)	23	31	13	27	—
I.S. Fe^{3+}	0.09	0.39	0.39	0.33	0.45
Q.S. Fe^{3+}	0.30	0.80	0.75	0.95	0.70
Width Fe^{3+}	0.31	0.45	0.30	0.31	0.25
Area Fe^{3+} (%)	6	6	6	6	4
Misfit (%)	−0.01	−0.04	0.19	−0.14	0.00
Uncertainty (%)	−0.01	−0.01	0.02	−0.02	0.00

* Recalculations based on microprobe data and stoichiometry.

Clinopyroxene

Mössbauer spectra of clinopyroxenes may often be difficult to interpret because of the additional complications posed by higher Fe^{3+} contents, exsolution, and inhomogeneity (Rossman, 1980). Petrographic (thin section) and microprobe examination of clinopyroxenes in the five

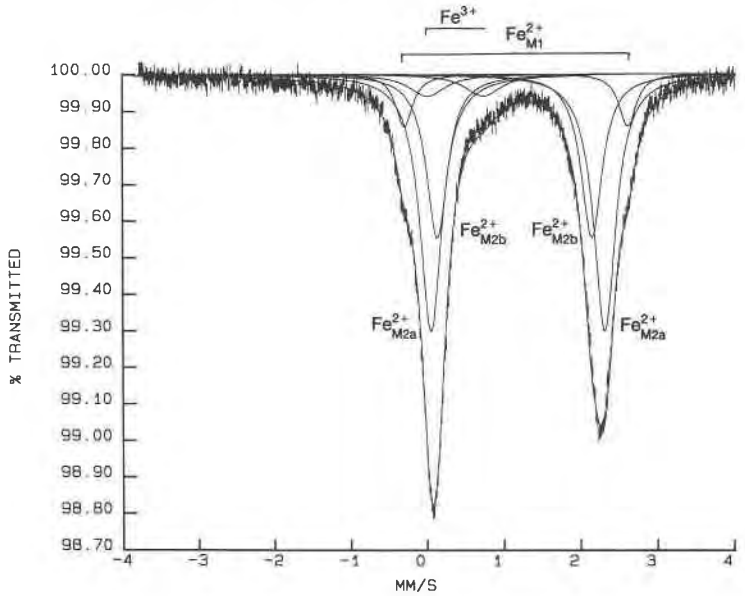

Fig. 4. Mössbauer spectrum of orthopyroxene (sample Ep-1-13). Most of the Fe in the orthopyroxene is found in the M2 doublets (two largest doublets). The outermost doublet, visible on the outer shoulders of the main peaks, represents Fe^{2+} in M1 sites. A small amount of Fe^{3+}, apparently in M1 sites, is also observed.

lherzolite xenoliths revealed exsolution in only one sample (H30-b2); that sample had about 5% of exsolved orthopyroxene and spinel that were not detected in its Mössbauer spectrum. The four other lherzolites contain homogeneous and unexsolved clinopyroxenes (App. I). The Fe^{3+} content of the lherzolite clinopyroxenes was roughly three times the amount observed in orthopyroxene (Fig. 6 and Table 4). Fe^{3+} ranged from a low of 12% in the Al Kishb sample (H30-b2) to a high of 22% in Ep-1-13 from Potrillo maar, occupying the octahedral M1 site in all samples. The Fe^{2+} contributions to the spectra again occur as (at least) two doublets. An outer doublet with $\Delta = 2.92$–2.95 mm/s is interpreted to represent occupancy of M1 octahedra by Fe^{2+}, while the inner doublet with smaller $\Delta = 1.94$–2.08 mm/s represents M2 octahedra. There is no obvious preference of Fe^{2+} for either M1 or M2 sites.

Peak width of the doublets fit to the clinopyroxene data

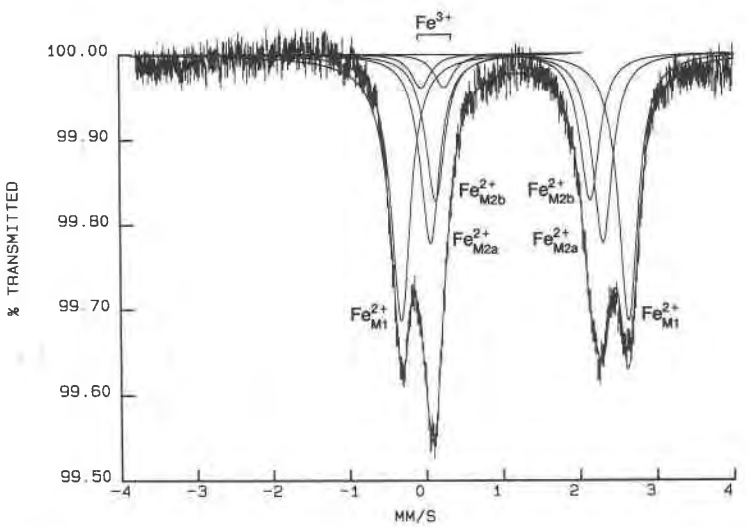

Fig. 5. The orthopyroxene separated from the Dish Hill peridotite (Ba-2-3) displays an unusually disordered Fe^{2+} distribution between M1 and M2 octahedral sites. In this sample, 41% of the total Fe is Fe^{2+} in the M1 site; 53% of the total Fe is Fe^{2+} in the two types of M2 sites. A small amount of Fe^{3+} (6% of the total Fe) is also present.

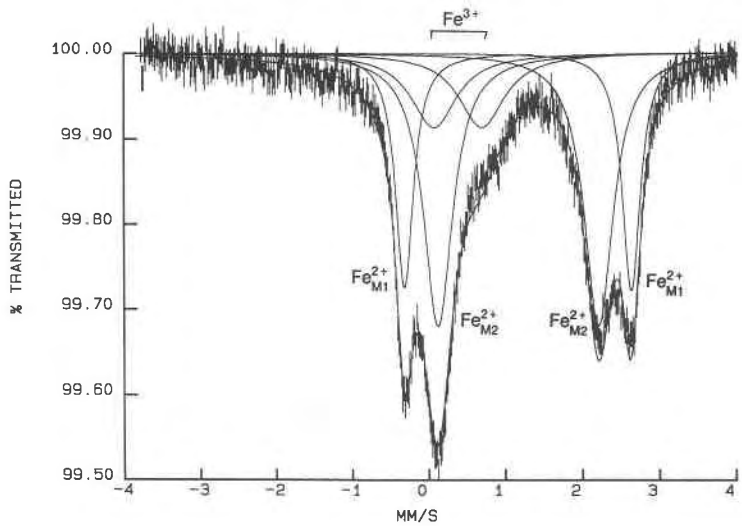

Fig. 6. Clinopyroxene spectrum of sample Sc-1-1 from San Carlos, Arizona. The outermost doublet represents Fe^{2+} in M1 sites, and the next smaller doublet is assigned to Fe^{2+} in M2. The small doublet in this sample represents Fe^{3+} in the octahedral M1 site.

are extremely variable; this is often taken as a sign of the presence of additional, potentially resolvable doublets that remain unfitted. Dual Fe^{2+}_{M1} doublets are sometimes observed in clinopyroxene spectra; this phenomenon was first interpreted by Dowty and Lindsley (1973) as arising from next-nearest-neighbor configurations, this time around the M1 site. In order to consider this model, eight peak fits were attempted on all samples in the data set (one Fe^{3+}, one Fe^{2+}_{M2}, and two Fe^{2+}_{M1} doublets). However, doublets in our room-temperature spectra were extremely overlapped in the eight peak fits, and satisfactory resolution and consistency in peak positions could not be obtained. We also observed that Fe^{3+} contents did not vary significantly as a function of the number of peaks used in a given model. Therefore only six peak fits are given in Table 4.

Discussion

Fe^{3+} calculated vs. Fe^{3+} measured

Detailed analysis of the crystal structures and Fe-site occupancies of the olivine, spinel, and pyroxene separates studied here provides insight into the validity of commonly accepted assumptions made with regard to Fe^{3+}. The most obvious conclusion that can be drawn from inspection of Tables 2–4 is that calculation of Fe^{3+} content of spinels and pyroxenes based on only stoichiometry and microprobe analyses is misleading, inconsistent, and (in all cases studied here) inaccurate. In the case of spinels, calculated Fe^{3+} values are generally (but not always) lower than measured Fe^{3+}. For pyroxenes, calculated Fe^{3+} values fluctuate widely and (apparently) randomly. For the pyroxenes in particular, such problems can probably be attributed to a lack of accuracy in the electron-microprobe data. The pyroxene Fe^{3+} calculations attempt to charge-balance 3+ tetrahedral cations with 1+, 2+, and 3+ octahedral cations while maintaining stoichiometry. Both these calculations are very sensitive to the assignment of tetrahedral and octahedral Al, which is in turn sensitive to the amount of Si. Therefore, errors in Si content (which is a difficult element to analyze accurately with the electron microprobe) can be propagated into the Fe^{3+} calculation and result in large errors. For example, a decrease of 1% in the SiO_2 content of a pyroxene, equivalent to a decrease of about 0.01 formula units of Si per six oxygens, can result in a tenfold increase in calculated Fe^{3+} (McGuire et al., 1989). Precision of modern electron microprobes is excellent, but extreme accuracy is difficult to obtain; even with careful calibration, accuracies of better than 1 wt% for SiO_2 are difficult to obtain. For this reason, models and thermobarometers based on calculated Fe^{3+} contents for minerals such as pyroxenes must be viewed with suspicion.

In contrast, Fe^{3+} values measured by Mössbauer spectroscopy are strikingly consistent. Fe^{3+} contents of orthopyroxenes are identical within analytical errors; Fe^{3+} in clinopyroxene covers only a relatively small range from 12 to 23%. Spinel Fe^{3+} contents range from a low of 22% to a high of 34% of the total Fe. Such demonstrated consistency of Fe^{3+} determinations further validates application of the Mössbauer technique to such studies, and should lead to enhanced consistency in f_{O_2} values derived from the data. Similar consistency of Mössbauer Fe^{3+} determinations was observed in a study of megacrysts from the Saudi Arabian, San Carlos, and Dish Hill localities (McGuire et al., 1989). Widely scattered calculated Fe^{3+} contents were observed for megacrysts with similar microprobe analyses and similar Mössbauer-determined Fe^{3+} contents.

Preliminary f_{O_2} calculations on these peridotites support the need for Mössbauer Fe^{3+} measurements and in-

TABLE 4. Summary of clinopyroxene data

	Dish Hill Ba-2-3	Potrillo maar Ep-1-13	Cima volcanic field Ki-5-31	San Carlos Sc-1-1	Al Kishb H30-b2
SiO_2	52.80	50.90	51.80	51.83	53.10
Al_2O_3	4.60	7.50	5.10	7.11	4.44
FeO	2.60	3.25	2.60	3.08	1.96
MgO	15.90	14.47	16.40	15.37	15.65
MnO	0.00	0.09	0.09	0.07	0.05
TiO_2	0.00	0.59	0.14	0.54	0.43
Cr_2O_3	0.75	0.70	0.75	0.67	1.23
CaO	21.30	19.55	21.40	19.56	21.57
Na_2O	1.30	1.56	1.07	1.41	1.23
Sum	99.25	98.61	99.35	99.64	99.66
Cations per six oxygens*					
Si	1.920	1.867	1.880	1.878	1.928
Al	0.197	0.324	0.218	0.304	0.190
Fe^{2+}	0.056	0.100	0.022	0.093	0.060
Fe^{3+}	0.023	0.000	0.057	0.000	0.000
Mg	0.862	0.791	0.886	0.830	0.847
Mn	0.000	0.003	0.003	0.002	0.002
Ti	0.000	0.016	0.004	0.015	0.012
Cr	0.022	0.020	0.022	0.019	0.035
Ca	0.830	0.769	0.832	0.759	0.840
Na	0.092	0.111	0.076	0.099	0.087
Sum	4.001	4.001	4.000	3.999	4.001
Wo	47.49	46.31	47.79	45.13	48.08
En	49.31	47.68	50.94	49.32	48.51
Fs	3.20	6.01	1.26	5.55	3.41
Fe^{3+} (calculated, %)	29	0	72	0	0
Fe^{3+} (Mössbauer, %)	17	23	18	21	12
I.S. M1	1.15	1.18	1.15	1.15	1.14
Q.S. M1	2.95	2.37	2.95	2.94	2.92
Width M1	0.26	0.44	0.27	0.28	0.34
Area M1 (%)	38	39	40	28	50
I.S. M2	1.15	1.14	1.15	1.15	1.13
Q.S. M2	2.08	1.94	2.07	2.08	2.06
Width M2	0.47	0.38	0.46	0.46	0.34
Area M2 (%)	45	38	44	51	38
I.S. Fe^{3+}	0.30	0.35	0.41	0.37	0.38
Q.S. Fe^{3+}	0.40	0.50	0.62	0.63	0.29
Width Fe^{3+}	0.87	0.63	0.58	0.72	0.34
Area Fe^{3+} (%)	17	23	18	21	12
Misfit (%)	−0.01	0.47	−0.16	−0.11	0.43
Uncertainty (%)	−0.01	0.04	−0.03	−0.03	0.04

* Recalculations based on microprobe data and stoichiometry.

dicate the potential errors generated by use of calculated Fe^{3+} values. Log f_{O_2} values were calculated (Eqs. 32 and 33 of Mattioli and Wood, 1988) for the spinel lherzolite samples by using both calculated and measured Fe^{3+} values. Use of calculated spinel Fe^{3+} values results in log f_{O_2} estimates of approximately −10 at 15 kbar and 900°C, in contrast with log f_{O_2} values of about −9 from calculations using measured Fe^{3+} in spinel and orthopyroxene. The Mössbauer measurements yield f_{O_2} values consistent with the FMQ stability region calculated by Mattioli and Wood (1986, 1988) for estimated compositions of Cr-rich diopside group spinel peridotites (Fig. 1). These results are far from the IW buffer region where Arculus and Delano's (1981) IOF measurements indicate the Cr-rich diopside group spinel peridotite region should lie.

Site occupancies of Fe

It was stated earlier that site occupancies in orthopyroxenes may provide clues to thermal history of our samples. It was noted that samples from the Dish Hill and Cima, California, localities contain high amounts of Fe^{2+} in the M1 site relative to the other orthopyroxene samples studied; no differences in major-element composition among any of the samples can be readily associated with this observation. Orthopyroxenes with such disordered Fe^{2+} contents have not previously been observed in such low Al compositions (J. R. Besancon, personal communication, 1988). However, it is obvious by inspection that the two California samples are fundamentally different from the other orthopyroxenes. Perhaps the explanation for this highly disordered Fe distribution is related to the presence of high heat flow in both regions. Both Dish Hill and Cima lie in the Basin and Range province, a region characterized by an elevated geotherm (Lachenbruch and Sass, 1977). Other peridotite xenoliths from those localities have textures that indicate melting of upper-mantle rocks, and textural and compositional evidence of metasomatism of upper-mantle peridotites (H. G. Wilshire, personal communication, 1988). Although our samples do not show the high Fe and Ti major-element concentrations commonly associated with metasomatism, they may still be showing its effects. Further study of additional samples from those localities is in progress to examine this phenomenon in more detail. Additional petrologic implications of the crystal-chemical data presented here are currently being considered (McGuire and Dyar, in preparation).

CONCLUSIONS

The Mössbauer investigation of coexisting phases in spinel lherzolites from localities at Dish Hill and Cima, California, San Carlos, Arizona, Potrillo maar, New Mexico, and Al Kishb, Saudi Arabia, has yielded new insight into their redox equilibria and crystal chemistry that can be summarized in five points:

1. Olivines in these rocks contain no detectable Fe^{3+}. Fe^{2+} doublets corresponding to both M1 and M2 octahedral sites are resolved in our room-temperature spectra, and resultant site occupancy ratios $Fe^{2+}_{M1}/Fe^{2+}_{M2}$ show variations from 1:1 to 3:1.

2. Spinel spectra are fit with four doublets corresponding to octahedral Fe^{3+}, octahedral Fe^{2+}, and two different types of tetrahedral Fe^{2+} sites. An alternate interpretation, assigning all three Fe^{2+} doublets to tetrahedral coordination, may also be possible given the large errors on the heavily overlapped spinel fits; however, the high-temperature origin of our samples favors the more disordered model. Calculation of log f_{O_2} values based on measured Fe^{3+} yields values close to the FMQ buffer at 15 kbar, in agreement with values estimated by Mattioli and Wood (1986, 1988) for Cr-rich diopside group spinel peridotites.

3. Orthopyroxene spectra also display four doublets

corresponding to Fe^{2+}_{M1}, Fe^{2+}_{M2} adjacent to divalent M1 sites, Fe^{2+} adjacent to partially trivalent M1 sites, and Fe^{3+} in predominantly octahedral M1 sites. Unusually high disorder of Fe^{2+} is observed in the two specimens from the California sites in the Basin and Range province and may be related to high heat flow in those regions.

4. Clinopyroxene data show that Fe^{2+} is distributed into both M1 and M2 octahedral sites, whereas Fe^{3+} may be either octahedral or tetrahedral.

5. Measured values of $Fe^{3+}/\Sigma Fe$ in all spinels and pyroxenes are consistent within each compositional range studied. In contrast, calculated Fe^{3+} values based solely on stoichiometry and electron-microprobe measurements are inconsistent and generally inaccurate.

Acknowledgments

We thank Bob Coleman for the loan of the Saudi Arabian xenolith, and Howard Wilshire for the loan of the xenoliths from the southwestern United States and unpublished analyses. John Wood is thanked for access to the Smithsonian Astrophysical Observatory microprobe. The support of NSF grants EAR-8709359 and DMR-8803179 (the latter from the Research Experience for Undergraduates program) is gratefully acknowledged. The assistance of Stuart Fuller, Matthew Hughes, Chryl Perry, and Kathleen Ward in data processing and of Stephen Waudby in manuscript preparation is greatly appreciated. The manuscript has benefited from reviews by R.J. Arculus, G.M. Bancroft, and H. Wilshire.

References cited

Amthauer, G. and Rossman, G.R. (1984) Mixed valence of iron in minerals with cation clusters. Physics and Chemistry of Minerals, 11, 37–51.

Annersten, H., Olesch, M., and Seifert, F.A. (1978) Ferric iron in orthopyroxene: A Mössbauer spectroscopic study. Lithos, 11, 301–310.

Anovitz, L.M., Essene, E.J., and Dunham, W.R. (1988) Order-disorder experiments on orthopyroxenes: Implications for the orthopyroxene geospeedometer. American Mineralogist, 73, 1060–1073.

Arculus, R.J., and Delano, J. W. (1981) Intrinsic oxygen fugacity measurements: Techniques and results for spinels from upper mantle peridotites and megacryst assemblages. Geochimica et Cosmochimica Acta, 45, 899–913.

Arculus, R.J., Dawson, J.B., Mitchell, R.H., Gust, D.A., and Holmes, R.D. (1984) Oxidation states of the upper mantle recorded by megacryst ilmenite in kimberlite and type A and B spinel lherzolites. Contributions to Mineralogy and Petrology, 85, 85–94.

Bancroft, G.M. (1967) Quantitative estimates of site populations in an amphibole by the Mössbauer effect. Physics Letters, 26A(1), 17–18.

——— (1969/1970) Quantitative site population in silicate minerals by the Mössbauer effect. Chemical Geology, 5, 255–258.

——— (1973) Mössbauer spectroscopy. Halsted Press, New York.

Bancroft, G.M., Burns, R.G., and Howie, R.A. (1967) Determination of the cation distribution in orthopyroxene series by the Mössbauer effect. Nature, 213, 1221–1223.

Bancroft, G.M., Osborne, M.D., and Fleet, M.E. (1983) Next-nearest neighbor effects in the Mössbauer spectra of Cr-spinels: An application of partial quadrupole splittings. Solid State Communications, 47(8), 623–625.

Banerjee, S.K., O'Reilly, W., Gibb, T.C., and Greenwood, N.N. (1969) The behavior of ferrous ions in iron-titanium spinels. Journal of Physics and Chemistry of Solids, 28, 1323–1335.

Besancon, J.R. (1981) Rate of cation disordering in orthopyroxenes. American Mineralogist, 66, 965–973.

Brown, G.E., Jr. (1982) Olivines and silicate spinels. In P.H. Ribbe, Ed., Orthosilicates (2nd edition). Mineralogical Society of America Reviews in Mineralogy, 5, 276–279.

Burns, R.G. (1981) Intervalence transitions in mixed valence minerals of iron and titanium. Annual Reviews of Earth and Planetary Science, 9, 345–383.

Bush, W.R., Hafner, S.S., and Virgo, D. (1970) Some ordering of iron and magnesium at the octahedrally coordinated site in a magnesium-rich olivine. Nature, 227, 1339–1341.

Canil, D., Virgo, D., and Scarfe, C.M. (1988) Oxidation state of spinel lherzolite xenoliths from British Columbia: A ^{57}Fe Mössbauer investigation. Carnegie Institution of Washington Year Book 87, 18–22.

Da Silva, E.G., Abras, A., and Sette Camara, A.O.R. (1976) Mössbauer effect study of cation distribution in natural chromites. Journale de Physique, Colloque, 37, C6-783–C6-785.

Da Silva, E.G., Abras, A., Speziali, N.L., and Sette Camara, A.O.R. (1980) Mössbauer effect study of natural chromites of Brazilian and Phillipine origin. Applied Physics, 22, 389–392.

Dehe, G., Seidel, B., Melzer, K., and Michalk, C. (1975) Determination of a cation distribution model of the spinel system $Fe_{3-x}Al_xO_4$. Physica Status Solidi, 81, 439–447.

Dowty, E., and Lindsley, D.H. (1973) Mössbauer spectra of synthetic hedenbergite-ferrosilite pyroxenes. American Mineralogist, 58, 850–868.

Dyar, M.D. (1984) Precision and interlaboratory reproducibility of measurements of the Mössbauer effect in minerals. American Mineralogist, 69, 1127–1144.

Eggler, D.H. (1983) Upper mantle oxidation state: Evidence from olivine-orthopyroxene-ilmenite assemblages. Geophysical Research Letters, 10, 365–368.

Ellis, D.J., and Green, D.H. (1979) An experimental study of the effect of Ca upon garnet-clinopyroxene Fe-Mg exchange equilibria. Contributions to Mineralogy and Petrology, 71, 13–22.

Evans, B.J., Ghose, S., and Hafner, S. (1967) Hyperfine splitting of ^{57}Fe and Mg-Fe order-disorder in orthopyroxene ($MgSiO_3$-$FeSiO_3$ solid solutions). Journal of Geology, 75, 306–322.

Fabries, J. (1979) Spinel-olivine geothermometry in peridotites from ultramafic complexes. Contributions to Mineralogy and Petrology, 69, 329–336.

Fatseas, G.A., Dormann, J.L., and Blanchard, H. (1976) Study of the Fe^{3+}/Fe^{2+} ratio in natural chromites. Journale de Physique, Colloque, 37, C6-787–C6-792.

Finger, L.W., and Virgo, D. (1971) Confirmation of Fe/Mg ordering in olivines. Carnegie Institution of Washington Year Book 70, 221–225.

Frey, F.A., and Prinz, M. (1978) Ultramafic inclusions from San Carlos, Arizona: Petrologic and geochemical data bearing on their petrogenesis. Earth and Planetary Science Letters, 38, 129–176.

Ghose, S. (1965) Mg^{2+}-Fe^{2+} order in an orthopyroxene, $Mg_{0.93}Fe_{1.07}Si_2O_6$. Zeitschrift für Kristallographie, 122, 81–99.

Grandjean, F., and Gerard, A. (1981) Mössbauer study of mixed valence spinels. Journal of Applied Physics, 52(3), 2164–2166.

Haggerty, S.E. and Tompkins, L.A. (1983) Redox state of Earth's upper mantle from kimberlitic ilmenites. Nature, 303, 295–300.

Harley, S.L. (1984) An experimental study of the partitioning of Fe and Mg between garnet and orthopyroxene. Contributions to Mineralogy and Petrology, 86, 359–373.

Jensen, S.D., and Shive, P.N. (1973) Cation distribution in sintered titanomagnetites. Journal of Geophysical Research, 78, 8474–8480.

Koseluk, R.A., Elliott, W.C., and Ulmer, G.C. (1979) Gas inclusions and f_{O_2}-T data for olivines from San Carlos, Arizona. EOS, 60, 419.

Kosoi, A.L., Malkova, L.A., and Frank-Kamenetskii, V.A. (1974) Crystal-chemical characterizations of rhombic pyroxenes. Soviet Physics and Crystallography, 19, 171–174.

Krizhanskiy, L.M., Nikitina, L.P., Khristoforov, K.K., and Yekimov, S.P. (1975) Distribution of Fe^{2+} and geometry of the cation oxygen polyhedra in the structures of orthopyroxenes at different temperatures (according to the data of Mössbauer spectroscopy). Geochemistry International, 1975, 54–62.

Lachenbruch, A.H., and Sass, J.H. (1977) Heat flow in the United States and the thermal regime of the crust. In J.G. Heacock, Ed., The Earth's crust: Its nature and physical properties. American Geophysical Union Geophysical Monograph Series, 20, 626–675.

Lumpkin, G.R., and Ribbe, P.H. (1983) Composition, order-disorder, and lattice parameters of olivines: Relationships in silicate, germanate, beryllate, phosphate, and borate olivines. American Mineralogist, 68, 164–176.

Marfunin, A.S. (1979) Spectroscopy, luminescence, and radiation centers in minerals. Springer-Verlag, New York.

Mattioli, G.S., and Wood, B.J. (1986) Upper mantle oxygen fugacity recorded by spinel lherzolites. Nature, 322, 626–628.

——— (1988) Magnetite activities across the $MgAl_2O_4$-Fe_3O_4 spinel join, with application to thermobarometric estimates of upper mantle oxygen fugacity. Contributions to Mineralogy and Petrology, 98, 148–162.

McGuire, A.V., Dyar, M.D., and Ward, K.A. (1989) Neglected Fe^{3+}/Fe^{2+} ratios: A study of Fe^{3+} content of megacrysts from alkali basalts. Geology, 17, 687–690.

Moats, M.A., and Ulmer, G.C. (1986) Interpreting IOF results for ilmenite-bearing xenoliths using Mössbauer spectroscopy. EOS, 67, 414.

Navrotsky, A., and Kleppa, O.J. (1967) The thermodynamics of cation distributions in simple spinels. Journal of Inorganic Nuclear Chemistry, 29, 2701–2714.

——— (1968) Thermodynamics of formation of simple spinels. Journal of Inorganic Nuclear Chemistry, 30, 479–498.

Nolet, D.A., and Burns, R.G. (1979) Ilvaite: A study of temperature dependent electron delocalization by the Mössbauer effect. Physics and Chemistry of Minerals, 4, 221–234.

O'Neill, H.St.C., and Wall, V.J. (1987) The olivine-orthopyroxene-spinel oxygen geobarometer, the nickel precipitation curve, and the oxygen fugacity of the Earth's upper mantle. Journal of Petrology, 28, 1169–1191.

Osborne, M.D., Fleet, M.E., and Bancroft, G.M. (1981) Fe^{2+}-Fe^{3+} ordering in chromite and Cr-bearing spinels. Contributions to Mineralogy and Petrology, 77, 251–255.

——— (1984) Next-nearest neighbor effects in the Mössbauer spectra of (Cr, Al) spinels. Journal of Solid State Chemistry, 53, 174–183.

Pasteris, J.D., and Wanamaker, B.J. (1988) Laser Raman microprobe analysis of experimentally re-equilibrated fluid inclusions in olivine: Some implications for mantle fluids. American Mineralogist, 73, 1074–1088.

Pike, J.E.N., and Schwarzman, E.C. (1977) Classification of textures in ultramafic xenoliths. Journal of Geology, 85, 49–61.

Press, S., Witt, G., Seck, H.A., Eonov, D., and Kovalenko, V.I. (1986) Spinel peridotite xenoliths from the Tariat Depression, Mongolia. I: Major element chemistry and mineralogy of a primitive mantle xenolith suite. Geochimica et Cosmochimica Acta, 50, 2587–2599.

Rossman, G.R. (1980) Pyroxene spectroscopy. In C.T. Prewitt, Ed., Pyroxenes. Mineralogical Society of America Reviews in Mineralogy, 7, 93–116.

Ruby, S.L. (1973) Why Misfit when you already have χ^2? In I.J. Gruverman, C.W. Seidel, and D.K. Dieterly, Eds., Mössbauer effect methodology, vol. 9, p. 277–305. Plenum Press, New York.

Sachtleben, Th., and Seck, H.A. (1981) Chemical control of Al-solubility in orthopyroxene and its implications on pyroxene geothermometry. Contributions to Mineralogy and Petrology, 78, 157–165.

Sawatzky, G.A., Van der Woude, F., and Morrish, A.H. (1968) Cation distributions in octahedral and tetrahedral sites of the ferrimagnetic spinel $CoFe_2O_4$. Journal of Applied Physics, 19, 1204–1206.

Seifert, F. (1983) Mössbauer line broadening in aluminous orthopyroxenes: Evidence for next nearest neighbors interactions and short-range order. Neues Jahrbuch für Mineralogie Abhandlungen, 148, 141–162.

Spencer, C.D., and Schroeer, D. (1974) Mössbauer study of several cobalt spinels using Co^{57} and Fe^{57}. Physical Review B, 9, 3658–3665.

Stanek, J., Hafner, S.S., and Sawicki, J.A. (1986) Local states of Fe^{2+} and Mg^{2+} in magnesium-rich olivines. American Mineralogist, 71, 127–135.

Stone, A.J., Parkin, K.A., and Dyar, M.D. (1984) STONE: A curve-fitting program for Mössbauer spectra. DEC User's Society Publication, 11-720, Marlboro, Massachusetts.

Ulmer, G.C., Grandstaff, D.E., White, D., Moats, M.A., Buntin, T.J., Gold, D.P., Hatton, C.J., Kadik, A., Koseluk, R.A., and Rosenhauer, M. (1987) The mantle redox state: An unfinished story? In E.M. Morris and J.D. Pasteris, Eds., Mantle metasomatism and alkaline magmatism. Geological Society of America Special Paper 215, 5–23.

Van Diepen, A.M., and Lotgering, F.K. (1977) Electron exchange between Fe^{2+} and Fe^{3+} on octahedral sites in spinels. Physica 86-88B, 961–962.

Virgo, D. (1972) ^{57}Fe Mössbauer analysis of Fe^{3+} clinopyroxenes. Carnegie Institution of Washington Year Book 71, 534–538.

Virgo, D., and Hafner, S.S. (1968) Re-evaluation of the cation distribution in orthopyroxenes by the Mössbauer effect. Earth and Planetary Science Letters, 4, 265–269.

——— (1969) Fe^{2+}-Mg order-disorder in heated orthopyroxenes by the Mössbauer effect. Mineralogical Society of America Special Paper 2, 67–81.

——— (1970) Fe^{2+}-Mg order-disorder in natural orthopyroxenes. American Mineralogist, 55, 201–223.

Ward, K.A., McGuire, A.V., and Dyar, M.D. (1988) Ferric iron content of megacrysts in alkali basalts. EOS, 69, 1483.

Wells, P.R.A. (1977) Pyroxene geothermometry in simple and complex systems. Contributions to Mineralogy and Petrology, 69, 129–139.

Wilshire, H.G., and Shervais, J.W. (1975) Al-augite and Cr-diopside ultramafic xenoliths in basaltic rocks from the western United States. Physics and Chemistry of the Earth, 9, 257–272.

Wood, B.J., Esperanca, S., and Virgo, D. (1988) Oxidation state of the upper mantle. Geological Society of America Abstracts with Programs, 20, A31.

Manuscript received November 30, 1988
Manuscript accepted May 24, 1989

Appendix 1. Petrographic descriptions

Textural descriptions follow the terminology of Pike and Schwarzman (1977).

H30-b2 Harrat al Kishb, Saudi Arabia. Mode: 10% Cpx, 20% Opx, 70% Olv, 1% spinel. Coarse-grained (2–5 mm) inequigranular, allotriomorphic-granular texture. Orthopyroxene contains exsolved clinopyroxene lamellae; clinopyroxene contains exsolved orthopyroxene and spinel.

Ba-2-3 Dish Hill, California. Mode: 15% Cpx, 30% Opx, 50% Olv, 5% spinel. Medium-grained (1–2 mm), equigranular-mosaic texture with slight foliation visible in hand sample. Minor kink bands in olivine. Pyroxenes are not exsolved.

Ki-5-31 Cima volcanic field, California. Mode: 10% Cpx, 25% Opx, 60% Olv, 5% spinel, traces of plagioclase. Medium-grained (1–2 mm), equigranular-mosaic to allotriomorphic texture. Pyroxenes not exsolved.

Sc-1-1 San Carlos, Arizona. Mode: 15% Cpx, 20% Opx, 65% Olv, 1–2% spinel. Medium-coarse-grained (1–4 mm), inequigranular, allotriomorphic-granular texture. Pyroxenes are not exsolved.

Ep-1-13 Potrillo maar, New Mexico. Mode: 15% Cpx, 25% Opx, 60% Olv, 1–2% spinel. Coarse-grained (1–5 mm), inequigranular, allotriomorphic-granular texture. Pyroxenes are not exsolved.